Neuropsychologia 48 (2010) 3145–3154

Contents lists available at ScienceDirect

Neuropsychologia

journal homepage: www.elsevier.com/locate/neuropsychologia

Probing the lifetimes of auditory novelty detection processes

Felipe Pegado[a,b,c], Tristan Bekinschtein[b,c,d], Nicolas Chausson[a], Stanislas Dehaene[c,e], Laurent Cohen[a,b,f], Lionel Naccache[a,b,f,*]

[a] AP-HP, Groupe hospitalier Pitié-Salpêtrière, Departments of Neurophysiology & Neurology, Paris, France
[b] INSERM, ICM Research Center, UMRS 975, Paris, France
[c] INSERM-CEA Cognitive Neuroimaging Unit | CEA/SAC/DSV/DRM/Neurospin center, Gif/Yvette cedex, France
[d] MRC-Cognition and Brain Sciences Unit, Cambridge, UK
[e] Collège de France, Paris, France
[f] Université Paris 6, Faculté de Médecine Pitié-Salpêtrière, Paris, France

ARTICLE INFO

Article history:
Received 9 November 2009
Received in revised form 19 June 2010
Accepted 22 June 2010
Available online 30 June 2010

Keywords:
ERP
MMN
P300
Novelty detection
Audition
Perception

ABSTRACT

Auditory novelty detection can be fractionated into multiple cognitive processes associated with their respective neurophysiological signatures. In the present study we used high-density scalp event-related potentials (ERPs) during an active version of the auditory oddball paradigm to explore the lifetimes of these processes by varying the stimulus onset asynchrony (SOA). We observed that early MMN (90–160 ms) decreased when the SOA increased, confirming the evanescence of this echoic memory system. Subsequent neural events including late MMN (160–220 ms) and P3a/P3b components of the P3 complex (240–500 ms) did not decay with SOA, but showed a systematic delay effect supporting a two-stage model of accumulation of evidence. On the basis of these observations, we propose a distinction within the MMN complex of two distinct events: (1) an early, pre-attentive and fast-decaying MMN associated with generators located within superior temporal gyri (STG) and frontal cortex, and (2) a late MMN more resistant to SOA, corresponding to the activation of a distributed cortical network including fronto-parietal regions.

1. Introduction

Auditory novelty detection can be fractionated into multiple processing stages indexed by distinct neural correlates. A large number of studies used the auditory oddball paradigm while recording scalp event-related-potentials to describe the series of successive ERP components sensitive to stimulus novelty. In this classic paradigm, a subject is actively detecting (e.g.: counting) the occurrence of rare auditory stimuli delivered among frequent ones. The dimension used to manipulate stimulus regularity is usually acoustic (e.g.: tone duration, tone pitch, tone timbre), but can be more abstract (e.g.: relative pitch position, rules deviant).

1.1. MMN and P3 complexes

Across a large number of studies three main findings have been reliably reported. First, the earliest auditory scalp ERP components, up to ~80–100 ms after tone onset, are insensitive to stimulus novelty. Second, the first ERP component sensitive to auditory novelty is a large negative component ("Mismatch Negativity" or MMN) occurring in a relatively large time-window ranging from 100 ms to 250 ms after tone onset among studies. This MMN seems to reflect an automatic process largely immune to attention and executive control (Tiitinen, May, Reinikainen, & Naatanen, 1994), but recent reports challenged this radical view by showing, in some situations, a certain sensitivity of MMN complex to manipulations of attention (Arnott & Alain, 2002; Muller, Achenbach, Oades, Bender, & Schall, 2002). Nevetheless, MMNs are observed during sleep (Atienza, Cantero, & Dominguez-Marin, 2002), in infants and neonates (Dehaene-Lambertz & Dehaene, 1994), and can even be observed in some comatose patients where they predict recovery of consciousness within the next days (Fischer, Luaute, Adeleine, & Morlet, 2004; Kane, Curry, Butler, & Cummins, 1993; Naccache, Puybasset, Gaillard, Serve, & Willer, 2005). The neural generators of this MMN complex are localized in bilateral superior temporal gyri (Bekinschtein et al., 2009; Liebenthal et al., 2003; Molholm, Martinez, Ritter, Javitt, & Foxe, 2005), and also possibly in frontal cortex (Giard, Perrin, Pernier, & Bouchet, 1990). Third, following the MMN a large positive complex is recorded around 300 ms after rare stimulus onset: the P300 or P3 component (Squires, Squires, & Hillyard, 1975; Sutton, Braren, Zubin, & John, 1965). This complex has been associated to working memory updating (Donchin &

* Corresponding author at: Hôpital de la Salpetriere, Clinical Neurophysiology Department, 47 Bd de l'hopital, F-7561 Paris Cedex 13, France.
E-mail addresses: lionel.naccache@psl.aphp.fr, lionel.naccache@wanadoo.fr (L. Naccache).

0028-3932/$ – see front matter © 2010 Elsevier Ltd. All rights reserved.
doi:10.1016/j.neuropsychologia.2010.06.030

Coles, 1988), and its late component (P3b) seems to index conscious access to auditory and visual novelty detection (Sergent, Baillet, & Dehaene, 2005). This P3 complex spans over time in a larger temporal window than MMN (~250–600 ms) and corresponds to the activation of a very distributed cortical network including associative cortices and parieto-frontal regions.

In the present work, we addressed the issue of the respective lifetimes of the cognitive processes at work during auditory novelty detection: how long can each of these processes maintain representations of past events? Answering this question would allow a better characterization of the distinct forms of memories engaged in novelty detection, from low-level echoic memory systems up to actively maintained central processes related to working memory and conscious processing. Theoretical models suggest that the P3 complex reflects, at least in part, a process of conscious access to a global neuronal workspace which has the ability to maintain information in a metastable reverberatory state, thus predicting that the P3 should have an arbitrary lifetime only limited by the subject's ability to remain attentive to the stimuli (Dehaene & Naccache, 2001). Conversely, simulations of networks of spiking neurons suggests that unless recurrent connections exceed a threshold, sensory-induced activation will decay exponentially with a time constant determined in part by internal noise and reverberation strength (Zylberberg, Dehaene, Mindlin, & Sigman, 2009). Thus we expected the MMN complex to show such decay, possibly with a shorter time constant for early sensory systems that receive less intense recurrent connections.

In addition to this theoretical goal, the issue of assessing lifetimes of perceptual representations is also of prime interest for medical purposes: probing the existence of long-lasting, actively maintained representations in an individual on a purely neurophysiological basis—that is to say without a behavioral measure, could help to probe the existence of conscious processing and working memory updating in non-communicating patients suffering from disorders such as comatose, vegetative state (VS), minimally conscious state (MCS) or conscious but paralyzed patients (e.g.: "locked in syndrome", severe amyotrophic lateral sclerosis (ALS) or severe "Guillain-Barré syndrome") (Laureys, Owen, & Schiff, 2004).

1.2. Manipulating SOA to probe lifetime of perceptual representations

An indirect way to explore this issue consists of manipulating the time delay between two successive stimuli, defined either as an SOA (Stimulus Onset Asynchrony) or as an ISI (Inter-Stimulus Interval). For each auditory novelty detection process, corresponding ERP correlates are predicted to vanish as soon as the SOA/ISI exceeds the time-window during which representations based on past auditory events are actively maintained. Note that the precise informational content of the representations stored in these memory systems is still open to inquiry and could correspond either to past perceptual representations, or to current predictions of stimulus expectancies according to a more Bayesian perspective (Friston, 2005; Garrido, Kilner, Stephan, & Friston, 2009).

Using this approach to investigate the cognitive process indexed by the MMN, Mantysalo and Naatanen (1987) showed that MMN was resistant to increasing ISIs up to 2 s, while no significant MMN could be observed for ISIs equal or superior to 4 s. However, Czigler, Csibra, and Csontos (1992) reported an MMN for an SOA of 7.2 s. Atienza et al. used a paradigm combining short fixed SOA trains of tones separated by variable silence interval. This paradigm allows the comparison of intra-train deviant MMN with inter-trains MMN (deviant occurring on the first stimulus of the train). They reported MMN for 9 s inter-train silences in awake subjects, while MMN vanished during REM-sleep for silences superior to 3 s (Atienza et al., 2002).

Part of this discrepancy concerning MMN lifetime might originate from the heterogeneous and dissociable nature of the multiple processes which are subtending the generic 'MMN'. Indeed, as early as 1987, Naatanen and Picton noted that N1 and MMN not only fall during overlapping time-windows, but also correspond to the net combination of at least 6 processes (Naatanen & Picton, 1987). A set of convergent results obtained across multiple brain-imaging methods (ERP, PET, EEG-fMRI, MEG, SEEG) reliably identified multiple neural generators of MMN within primary and secondary auditory cortex (Naatanen , Tervaniemi , Sussman , Paavilainen, & Winkler, 2001), with variable localization depending on which feature of the sound changes (Levanen, Hari, McEvoy, & Sams, 1993). Additional sources have been reported in frontal cortex (Doeller et al., 2003; Giard et al., 1990; Rosburg et al., 2005), right inferior parietal cortex (Levanen, Ahonen, Hari, McEvoy, & Sams, 1996), and in subcortical primary and non-primary thalamic structures both in animal models (e.g.: guinea pig see (Kraus, McGee, Nicol, & King, 1994)) and in humans. Multiple sources of the MMN have also been reported during infancy (Dehaene-Lambertz, 2000). The respective temporal and attentional characteristics of each of these sub-components might differ as previously shown for the frontal component of MMN which occurs later in time than the temporal MMN (Opitz, Rinne, Mecklinger, von Cramon, & Schroger, 2002), and is affected by attentional load while the temporal MMN is not (Restuccia, Della Marca, Marra, Rubino, & Valeriani, 2005).

In sharp contrast with the MMN, P3 components seem to be much more resistant to SOA/ISIs and much more sensitive to attentional manipulations, suggesting a close relationship with conscious working memory, the content of which can be actively maintained for a virtually unlimited duration. In accordance with this concept, Polich et al. elicited P3 in a "single-trial" paradigm during which a single stimulus type is played throughout the experiment but with extremely long ISIs around tens of minutes (Polich, Eischen, & Collins, 1994; Polich & Margala, 1997).

Here, we probed the respective lifetimes of auditory novelty detection ERP correlates in a group of normal controls. We used a standard oddball paradigm with 3 distinct SOAs (600 ms, 1000 ms, 2000 ms) in distinct experimental blocks. In Experiment 1 we recorded high-density (128 electrodes) scalp ERPs in order to finely describe the spatio-temporal characteristics of MMN and P3 complexes. Experiment 2 replicated main findings of Experiment 1 using a rudimentary setting (3 active electrodes) more compatible with standard clinical settings in Intensive Care Units (ICU).

2. Material and methods

2.1. Subjects

Thirty six neurologically normal subjects with no auditory impairment (16 males; 18–38 years old; median age = 24.5; mean age = 25.3) gave their informed consent and volunteered to this study. Twelve subjects participated to Experiment 1 (high-density scalp ERPs) while the remaining 24 subjects participated to Experiment 2 ("bedside like" scalp ERPs with 3 active needle electrodes). Experiments were approved by the Ethical Committee of the Salpêtrière hospital.

2.2. Stimuli and procedure

Each subject was exposed to three experimental blocks the order of which was balanced across subjects using a "Latin Square" design (2 subjects included in Experiment 2 were discarded for partial data loss). Each block was defined by a specific fixed SOA: 600 ms, 1000 ms or 2000 ms. In each block, binaural tones were pseudo-randomly delivered (+80 dBl, 40 ms duration, frequent in 85% of

trials, rare in 15% of trials) with the given SOA. Half of the subjects were stimulated with a 1000 Hz tone as the frequent stimulus and with a 2000 Hz tone as the rare stimulus, while the other half of the population was stimulated with the inverse pattern of tones probability. Each block consisted of several mini-blocks of similar duration (~5 min) separated by short pauses. Task instruction was to count the number of rare stimuli and verbal responses were collected at the end of each mini-block. Number of rare trials was fixed for each SOA (108, 110 and 120, respectively) in order to avoid a systematic constant response. Number of experimental mini-blocks for each SOA varied from 2 (SOA 600 ms), to 4 (SOA 1000 ms) and 6 (SOA 2000 ms). Mini-block duration varied from 220 s (SOA 600 ms), 200 s (SOA 1000 ms) and 240 s (SOA 2000 ms).

2.3. EEG recording and ERP analysis

2.3.1. Experiment 1: high-density scalp ERPs

ERPs were sampled at 250 Hz with a 128 electrode geodesic sensor net (EGI, Oregon, USA) referenced to the vertex. We rejected voltages exceeding ±100 μV, transients exceeding ±150 μV, or electro-oculogram activity exceeding ±70 μV. Trials were then segmented from −100 ms to +500 ms relative to the onset of the sound. Bad channels were interpolated using a spherical splines interpolation method (Perrin, Pernier, Bertrand, & Echallier, 1989). Trials with more than 20% bad channels were rejected. The remaining trials were averaged in synchrony with stimulus onset, digitally transformed to an average reference, band-pass filtered (0.5–40 Hz) and corrected for baseline over a 100 ms window before stimulus onset. All those processing stages were performed in the EGI Waveform Tools Package. Matlab 7.0 (Natick, MA, USA) scripts were used to compute sample-by-sample paired *t*-tests with a double criterion of: $p < .01$ for at least 10 consecutive samples. Grand-average ERPs, and voltage topographical maps were performed with Cartool software programmed by Denis Brunet (http://brainmapping.unige.ch/Cartool.htm).

Latencies of ERP effects were estimated by identifying the first significant time sample of sample-by-sample *t*-tests between rare and frequent trials (Luck, 2005).

Comparison of voltage amplitudes across SOAs were performed by using an ANOVA approach. We defined the four events of interest (early MMN, late MMN, P3a and P3b) by inspecting the time course of scalp voltage maps of the rare minus frequent subtraction collapsed across the 3 SOAs. For each effect a region of interest (10 contiguous electrodes: Fz centered for early MMN, Cz centered for late MMN and P3a, Pz centered for P3b), and a 64 ms width time-window were defined (96–160 ms for early MMN, 164–228 ms for late MMN, 320–384 ms for P3a, and 400–464 ms for P3b). Voltage differences between rare and frequent trials were then averaged for each effect, for each SOA and for each subject. We then ran an ANOVA (SOA(3) × Subjects (11)) for each event of interest, with subject factor declared as a random factor.

2.4. Multiple regression analysis

We defined the four events of interest (early MMN, late MMN, P3a and P3b) by inspecting the time course of scalp voltage maps of the rare minus frequent subtraction collapsed across the 3 SOAs. For each event the relevant time sample was identified visually (128 ms, 192 ms, 320 ms and 416 ms, respectively), and the corresponding regressor was defined as a 128 voltage values vector. Then we ran a multiple linear regression analysis for each time sample and for each SOA, using a model defined by these four regressors of interest in addition to a constant regressor. The time course of each regressor of interest was then extracted (beta coefficients), and plotted (see Fig. 3). In order to assess the significance of amplitude and latency effects across SOAs, similar regressions analyses were run for each subject and for each SOA, and beta coefficients were submitted to analyses of variance.

For source estimation, cortical current source density mapping was obtained using a distributed model consisting in 10,000 current dipoles. Dipole locations and orientations were constrained to the cortical mantle of a generic brain model built from the standard brain of the Montreal Neurological Institute using the BrainSuite software package. This head model was then warped to the standard geometry of the sensor net. The warping procedure and all subsequent source analysis were processed with the BrainStorm software package (http://neurimage.usc.edu/brainstorm). EEG forward modelling was computed with an extension to EEG of the overlapping-spheres analytical model. Cortical current maps were computed from the EEG time series using a linear inverse estimator (weighted minimum-norm current estimate or WMNE, see Baillet, Moscher, and Leahy (2001) for review).

2.4.1. Experiment 2:3 active electrodes ERPs

The P8 Medatec system (Bruxelles, Belgium) was used to deliver the acoustic stimulation, to record and digitize at 1000 Hz EEG epochs of 500 ms including a 100 ms-long baseline from Cz and Pz referenced to the left mastoid, to filter the signal (time constant = 0.03 s; low-pass cut-off = 100 Hz), and to automatically reject epochs with an amplitude exceeding ±100 μV). Individual trials were then exported and processed in Matlab 6.5 (Natick, MA) to reject frequent trials occurring immediately after a rare trial, to apply a direct-form II transposed filter (low-pass filter = 70 Hz), to average the signal, and to perform sample-by-sample *t*-tests, with criteria of a minimum of 10 consecutive *p* values lower than 0.05. We set the *p* value threshold higher than in Experiment 1 because the number of multiple comparisons performed was much lower in Experiment 2 (32250 vs 1000).

Latencies and amplitude analyses were performed similarly as in Experiment 1.

3. Results

3.1. Experiment 1

3.1.1. Behavior

Behavioral performance was close to perfection: correct performance rate (number of detected stimuli/total number of stimuli) calculated for every SOA ranged from 92% to 100% (mean = 98%, standard deviation = 2.6%), with the exception of one subject who performed very poorly (68% correct responses). Post-experiment debriefing identified a partial sleep deprivation in this subject. She was discarded before further analyses. No significant difference was observed across SOAs: 98% for SOA of 600 ms, 97% for SOA of 1000 ms and 97% for SOA of 2000 ms ($F(2,20) = 2.3$; $p = 0.12$).

3.2. Event-related potentials

3.2.1. Correlates of novelty detection: MMN and P3 complexes

For each subject and for each SOA, we subtracted mean ERPs elicited by rare stimuli from mean ERPs elicited by frequent stimuli, and calculated the grand-averages of these subtractions across subjects. Inspection of scalp topographies and of statistical maps (see Fig. 1) revealed four main effects of novelty detection: the early and late MMN, and the P3a and P3b ERP components.

First, an anterior central negativity corresponding to the MMN complex was observed between 96 ms and 224 ms after sound onset, and could be divided in an early MMN (peaking at 128 ms [96–160 ms]), and late MMN (peaking at 192 ms [164–224 ms]). The early part of this complex was an anterior negativity centered around Fz, while its late part was vertex centered (see Fig. 3 and

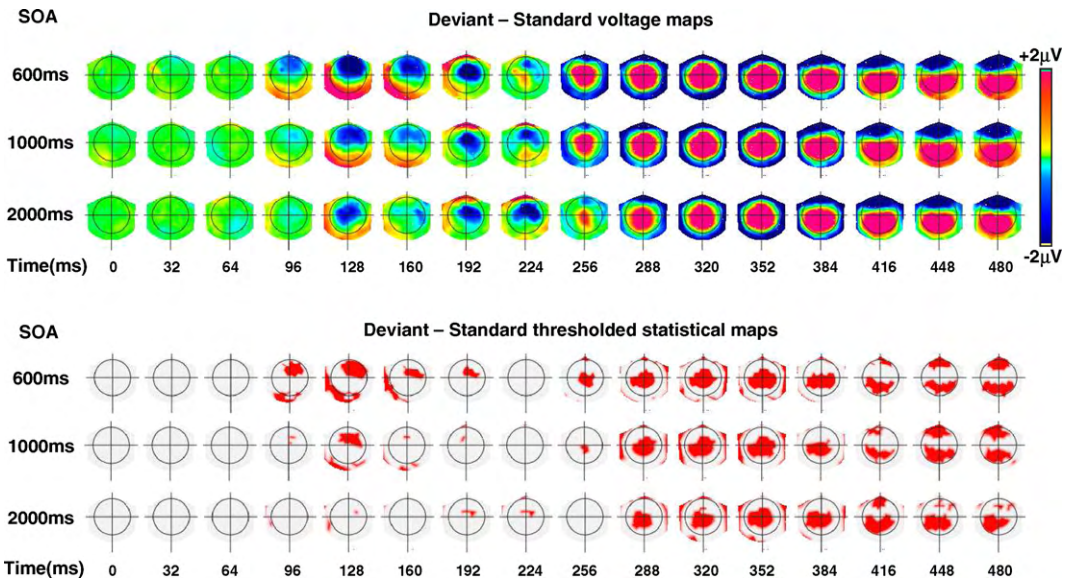

Fig. 1. Scalp topographies of auditory novelty detection effects. Top panel: voltage scalp topographies of deviant minus standard grand-averaged ERPs are plotted for each SOA, and reveal a succession of 4 events: an early MMN decaying over SOA, followed by a late MMN showing a delay effect, and a P3 complex including a P3a component characterized by a vertex centered positivity, and a P3b component defined as a positivity centered around parietal regions. Bottom panel: corresponding statistical topographies are plotted. Red maps indicate the presence of a significant effect satisfying a double-criterion on a sample-by-sample Student's *t*-test: *p* value inferior to 0.01 for at least 10 consecutive samples. This statistical figure confirms the decay of early MMN across SOA and the stability of the P3 complex.

regression analysis below). Moreover, while the early MMN progressively decreased across SOAs ($F(2,20) = 11.9$; $p < 10^{-3}$), the "late MMN" resisted to SOAs ($F(2,20) = 0.3$; $p = 0.7$). This amplitude modulation of the early MMN by the SOA was associated to a small delay effect on latencies (estimated with a *t*-test method (Luck, 2005)): early MMN onset was estimated at 96 ms for the SOA 600 ms, and 104 ms for the SOA 1000 ms, while no early MMN could be detected for the longest SOA.

Visual inspection of ERPs elicited by standard and by rare sounds revealed that the progressive vanishing of the early MMN across SOAs corresponded to a response change to standard stimuli rather than to a change to rare stimuli (see Fig. 3, left inferior panel). We confirmed this result by running an ANOVA with the following design: subject (11) × condition (2) × SOA (3) on voltage averaged across 10 contiguous electrodes around Fz and across 96–160 ms (see Section 2). This analysis replicated the vanishing of MMN across SOAs (interaction between SOA and condition, ($F(2,20) = 6.9$; $p = 0.009$), but most importantly showed that while response to rare sounds was not affected by SOA ($p = 0.5$), a strong SOA effect was observed in response to frequent sounds ($p < 10^{-4}$).

Second, novelty detection was also associated with a large central positivity (P3 complex) ranging from ~250 ms up to the end of the epoch (500 ms). Latency of the onset of this P3 varied with SOA: the shortest the SOA, the earliest the P3 onset (240 ms, 256 ms, 268 ms, respectively). This P3 complex could be divided in an early P3a component corresponding to a vertex centered positivity and in a later P3b component characterized by a classical posterior Pz-centered scalp topography (see Figs. 1 and 3). Amplitudes of both the P3a and P3b components were not affected by the SOA (*F*-test *p* values > 0.2).

3.2.2. Delay effect of the late MMN–P3a transition

We reported a delay effect of the P3a component across SOAs. In order to better describe the significance this finding, we performed two additional analyses taking advantage of two global measures of our experimental effects: global field power (GFP) and scalp topographies.

Inspection of GFP curves of the rare minus frequent sounds subtractions calculated for each SOA confirmed the existence of a progressive delay of the transition between late MMN and P3a (see Fig. 2). According to this measure, the onsets of the P3a topography were delayed by a progressive increase of ~10 ms between each the 3 SOAs. Note that this estimation was very close to the estimation of ~14 ms calculated with the precedent method. The absolute values of P3a latency were found a bit earlier (224 ms, 236 ms, 244 ms, respectively) than with the single-electrode *t*-test method, most probably because this global measure taking advantage of the global variance of the EEG signal across the 128 electrodes can be more sensitive to the onset of distributed effects, and detect them before they reach a significant values under each electrode. In order to better assess the significance of this effect observed on grand-averaged GFP curves, we computed individual GFP values for each SOA and for each subject. We then identified the minimal values of the each GFP within the 200–300 ms time-window indicated in Fig. 2. These values were then submitted to a subject (11) × SOA(3) ANOVA, with subject declared as a random factor. This analysis confirmed the significance of this delay effect across SOAs ($F(2,20) = 25.7$; $p < 10^{-4}$), and all two-by-two post hoc *t*-tests were significant (all *p* values <0.01).

The dynamics of scalp topographies of these ERP effects were better assessed by using a multiple linear regression approach. In this additional analysis we used 4 topography templates enabling us to probe the respective dynamics of early and late MMN but also of P3a and P3b components of the P3 complex (see Section 2). This regression model confirmed the existence of a large effect of SOA modulating the amplitude of the early MMN (see Fig. 3). Sample-by-sample ANOVAs with SOA(3) × Subjects (11) performed on the temporal window of interest (see Fig. 1), confirmed the significance of this amplitude modulation effect (12 successive samples from 116 ms to 165 ms with *p* value < 0.05). This analysis also confirmed the existence of a delay effect of the SOA on the onset of the P3a (14 successive samples from 260 ms to 312 ms with *p* value < 0.05 both for the main effect of SOA and for a linear contrast [−1 0 1]), and revealed a similar delay effect on P3b components (10 successive samples from 340 ms to 376 ms with *p* value < 0.05 both for the main effect of SOA and for a linear contrast).

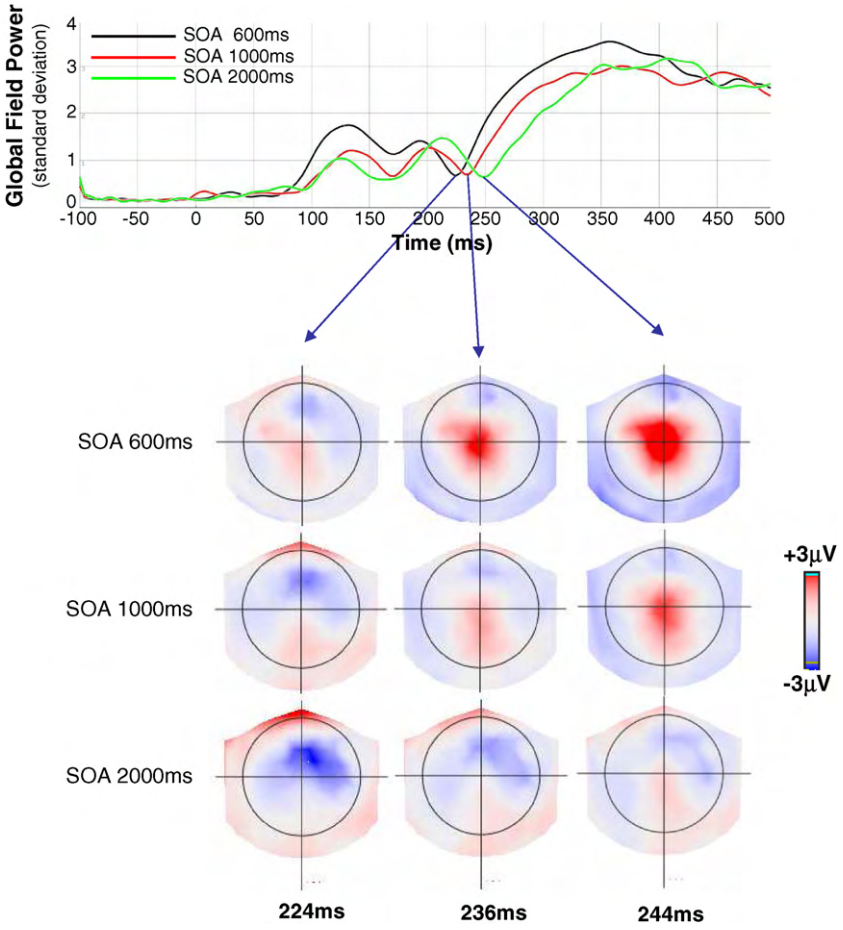

Fig. 2. Delay effects of SOA on MMN closure and P3 onset. Top panel: global Field Power, an index of signal variance, is plotted over time for each SOA. While a modulation of EEG variance by SOA is visible during the time-window of early MMN, a delay effect is apparent for the closure of MMN (see blue arrows pointing to the bottom panel), and for the rise-up of P3 component. Bottom panel: a focus on scalp topographies surrounding MMN closure and P3 onset reveals that while P3 onsets around 224 ms for the shortest SOA (600 ms), a late MMN is still visible for longest SOAs (1000–2000 ms). Late MMN is delayed, as is the P3 onset (diagonal of this 3 × 3 plotting).

3.2.3. Brain sources of MMN and P3 components

In order to better assess the respective neural dynamics of these four neural events (early and late MMN, P3a and P3b), and their differential sensitivity to SOA, we estimated their corresponding brain sources (see Fig. 4). Early MMN, which was best observed in the shortest SOA condition (600 ms), was associated with the activation of a rather focal cortical network including bilateral STG in addition to frontal sources, in particular in the right dorsolateral prefrontal cortex, as initially proposed by Giard et al. (1990). In close agreement with surface voltage findings, the early MMN disappeared at the longest SOA (2000 ms). Late MMN was associated with a distinct cortical pattern of activations including medial regions of the superior frontal gyrus in both hemispheres, in addition to fronto-polar cortices, and without visible activation of primary auditory regions. In order to better characterize the differences of spatial patterns of activation between early and late MMN, we focused on the 'SOA 600 ms' condition (left column of Fig. 4), where both early and late MMN could be observed. We defined two bilateral cortical regions of interests (ROIs) in the STG and mesio-frontal cortices respectively. We averaged source signal across each ROI, for each subject, across the relevant time-window (early MMN, late MMN). We then ran the following ANOVA: Subject (11) × ROI(2) × time-window(2), with subject as a random factor. We observed a strong ROI × time-window interaction ($F(1,10) = 16.6$; $p = 0.002$), corresponding to a strong increase of neural activity in mesio-frontal cortex ROI between early and late MMN ($p = 0.004$), while level of neural activity remained stable in the STG ($p = 0.4$). Note however, that this estimation of the spatial sources of late MMN remains largely speculative, due to the absence of validation of our results with another neurophysiological method endowed with a more robust spatial resolution, such as fMRI or intracranial recordings. However, the mere existence of spatial differences between estimated sources of the early MMN and late MMN is informative, and supports the distinction we propose between these two ERP components. Finally, P3 complex was associated to a large cortical network of activations, including in particular fronto-parietal regions, as commonly observed in the literature (Bekinschtein et al., 2009; Sergent et al., 2005).

3.3. Experiment 2

3.3.1. Behavior

Each of the subjects performed extremely well on the rare-stimuli counting task, for each of the three SOA conditions (0–2 errors for each block). Correct performance rate calculated for every SOA ranged from 91% to 100%. No difference was observed across SOAs: 98.6% for 600 ms; 97.6% for 1000 ms; 98.1% for 2000 ms ($F(2,46) = 1,0$; $p = 0.4$).

3.4. Event-related potentials

3.4.1. Probing these effects at bedside

The aim of Experiment 2 was to capture some of the key findings of Experiment 1 using a more rudimentary recording setting with

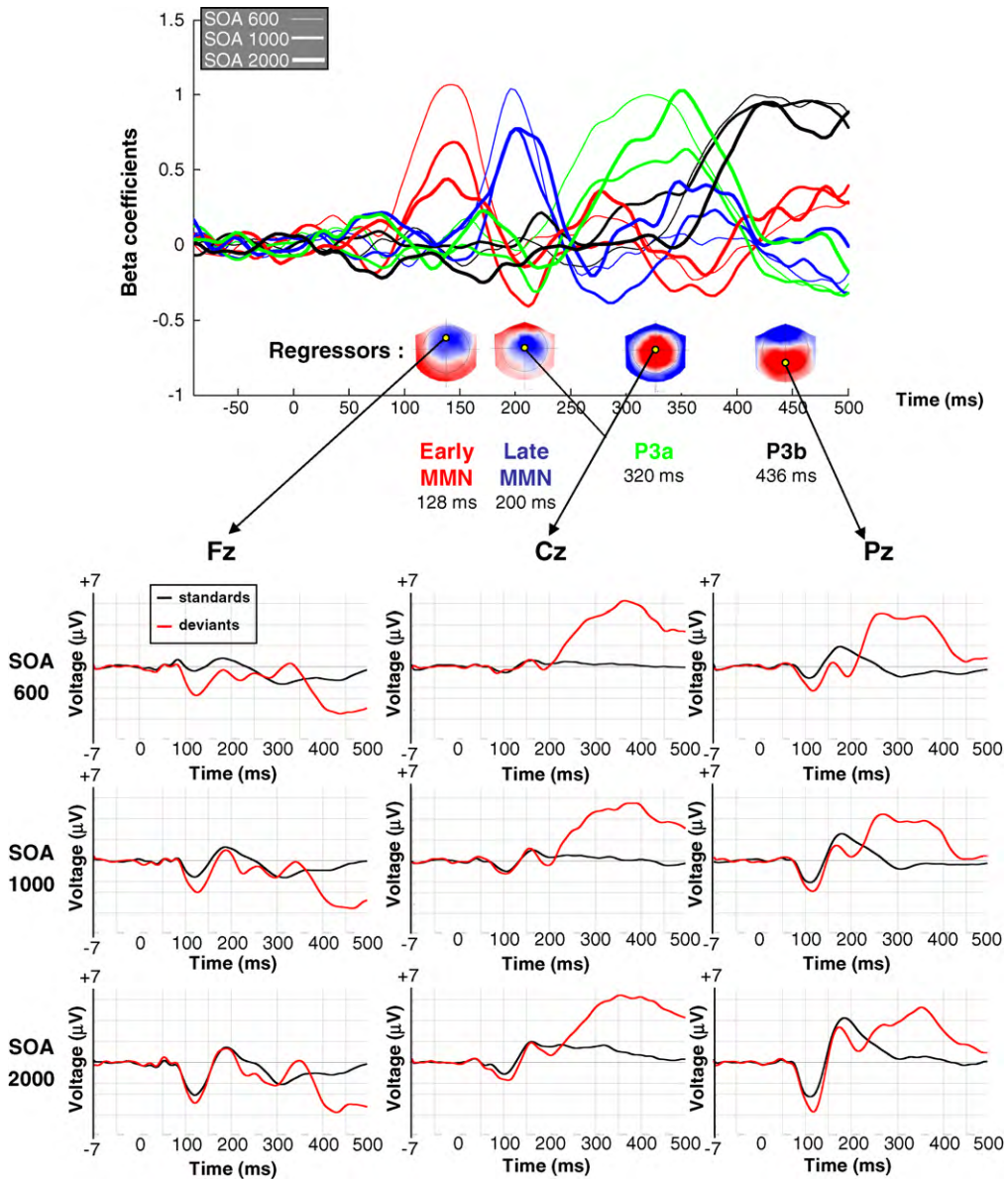

Fig. 3. Regression approach and representative ERPs. Top panel: grand-averaged subtracted ERPs (deviant-standard) of each SOA are modeled by a multiple linear regression using a constant and 4 vectors of interest corresponding respectively to early MMN, late MMN, P3a and P3b. The beta coefficients of each of these regressors are plotted over time for each SOA. Again, early MMN shows a modulation effect by SOA, while later events show a delay effect, including the late P3b component. Bottom panel: representative ERPs from middle line electrodes (Fz, Cz, Pz) are plotted for each SOA.

much poorer spatial sampling (3 active electrodes: Cz-A1 & Pz-A1), more compatible with widely used EEG recording systems in ICU. At the shortest SOA (600 ms), four ERP effects were observed: first, an early MMN spanning from 114 ms to 137 ms, followed by a positivity ranging from 147 ms to 185 ms and then by a P3 component followed by a late negativity (see Fig. 5). For the two longer SOAs (1000 ms and 2000 ms), neither the early MMN nor the following positivity reached the level of significance, but visual inspection of mean ERPs suggested a progressive attenuation of these two components with SOAs. Only the P3 response and the late negativity were present at the 3 SOAs. Latency of the P3 response slightly increased from 250 ms to 252 ms and 257 ms across SOAs. Given the poor spatial resolution of this recording setting with only two active derivations, we restricted amplitudes analyses to the two well defined ERP events: the early MMN and the P3 response. For each of these two effects, voltages were averaged across 40 ms temporal windows (100–140 ms for the early MMN, and 360–400 ms for the P3a). While main effect of SOA on the early MMN was not significant ($F(2,46) = 2.0$; $p = 0.2$), a linear contrast confirmed the existence of a progressive decrease of this ERP component across SOAs ($p = 0.04$). In sharp contrast, the P3 component was unaffected by the SOA ($p = 1$).

4. Discussion

In this study we investigated the impact of SOA on the distinct ERP correlates of novelty detection processes during an active version (counting task) of the traditional auditory oddball paradigm. During Experiment 1 we used a high-density EEG system allowing us to provide a fine description of the spatio-temporal dynamics of these effects, and Experiment 2 was designed to replicate Experiment 1 using a very rudimentary system compatible with clinical testing at bedside. Taken together our results confirm and precise previous results, and also provide original findings relevant to the understanding of cognitive processes at work during conscious and non-conscious novelty detection.

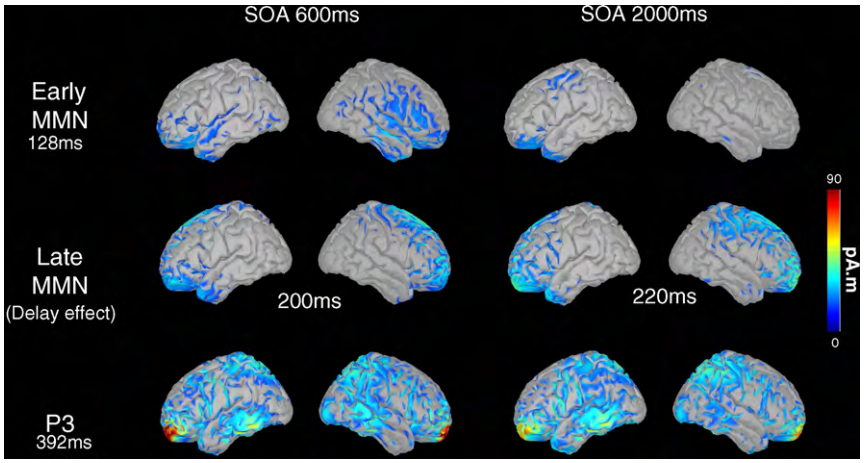

Fig. 4. Cortical sources of auditory novelty effects. Activations are expressed in terms of dipole current amplitude (pA/m), with a threshold at 20% of the maximal value indicated on the scale, and are plotted for the two extreme SOAs (600–2000 ms), at 3 representative times: early MMN (128 ms) is mostly associated with bilateral STG and frontal activations, while late MMN (200 ms and 220 ms due to the delay effect) correlates with a distinct pattern of sources including frontal poles and midline frontal structures. P3 (392 ms) sources delineate a distributed fronto-parietal network.

4.1. MMN and P3 complexes

In close accordance with the abundant existing literature related to this topic (see for reviews: Naatanen et al., 2001; Donchin & Coles, 1988), we observed two main correlates of novelty detection: an early anterior central MMN complex spanning from 90 to 220 ms after sound onset, followed by a vertex-centered P3 long-lasting complex spanning from around 250 ms and still present at the end of the epoch of interest (480 ms). As previously described, MMN amplitude decreased when SOA increased (Mantysalo & Naatanen, 1987), thus supporting the prevailing view which considers this ERP component as reflecting a fast decaying echoic memory process. Our finding that decrease of early MMN across SOAs mostly corresponded to a change in response to standard sounds, rather

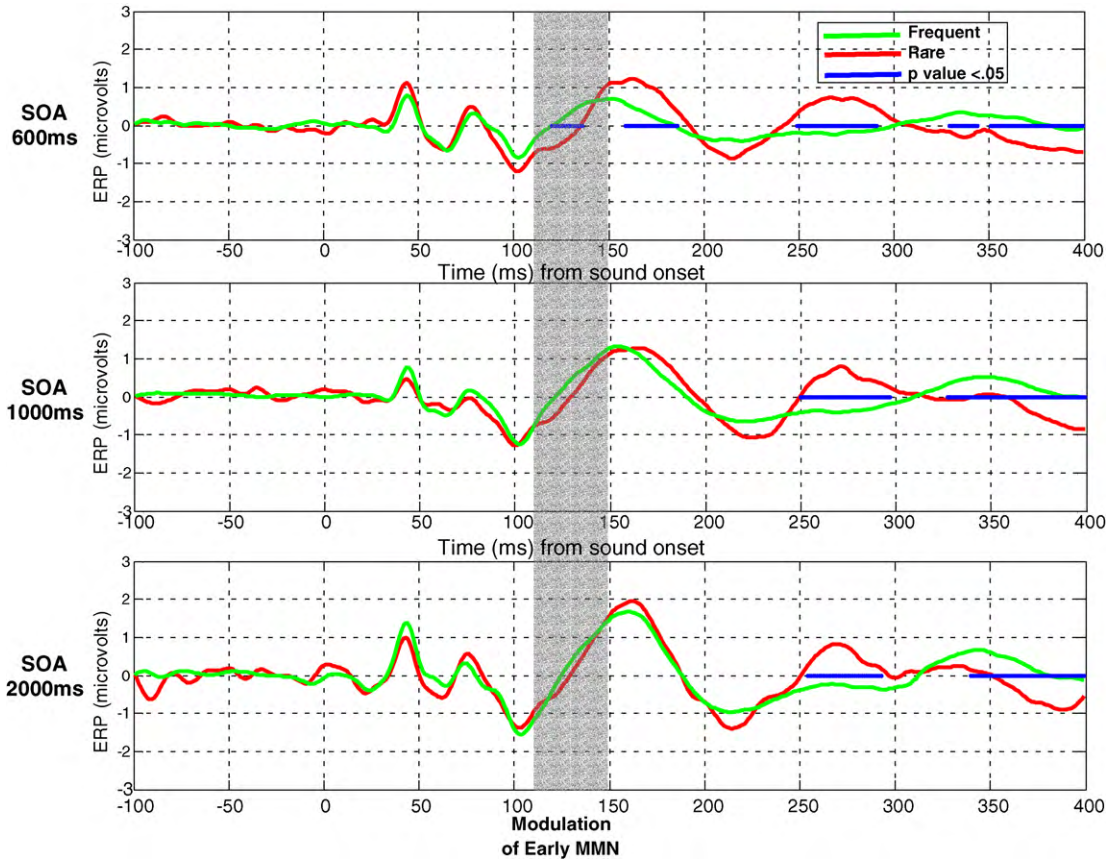

Fig. 5. Application to a basic EEG recording system. For each SOA, frequent (green) and rare (red) grand-averaged ERPs (Cz-A1 bipolar derivation) are plotted against time. Significant differences between the two conditions are indicated by blue dots (a minimum of 10 successive samples with Student's *t*-test *p*-value < 0.05). The basic EEG recording setting used here (Cz-A1 & Pz-A1 derivations) replicated the 3 main findings of Experiment 1 using high-density scalp recordings: (1) early MMN decayed across SOAs, (2) P3 onset was progressively delayed and (3) P3 complex was remarkably stable across SOAs. (For interpretation of the references to color in this figure legend, the reader is referred to the web version of this article.)

than to deviant sounds is highly compatible with the concept of very short term echoic memory. Consider an echoic memory system responding actively to any stimulus which differs from the stimuli delivered during the last second. As soon as the SOA will exceed the span of this echoic memory (e.g.: 1 s), this system will respond actively to any stimulus, including to a standard stimulus. Given that MMN is most commonly observed as a subtraction of neural responses elicited by rare and frequent stimuli, the vanishing of MMN across SOAs is often interpreted in terms of silencing of a novelty detection system. Our results show that the vanishing of the MMN corresponds actually to the very opposite phenomenon: all stimuli (rare & frequent) are processed as new stimuli by this novelty detection system once the SOA exceeds its memory span, and therefore the subtraction between responses elicited by rare and frequent stimuli tends to zero.

In sharp contrast, P3 complex was remarkably stable across the 3 SOAs, as could be expected from a working-memory related central process associated to active maintenance of perceptual information. Also, cortical sources of these effects confirmed previously observed findings: the early part of the MMN complex (~90–160 ms) originated from the activation of a confined network, the epicenters of which were located within bilateral STG and frontal cortices. Note that the presence of a frontal generator of the early MMN supports previous empirical reports (Bekinschtein et al., 2009; Giard et al., 1990). In sharp contrast with these focal brain activations, cortical sources of the P3 complex delineated a large cortical network including prefrontal, parietal and temporal areas, as observed in many studies (Bledowski et al., 2004; Clarke, Halgren, & Chauvel, 1999; Halgren, Marinkovic, & Chauvel, 1998; Mantini et al., 2009) and as predicted by the global workspace model of conscious processing (Dehaene & Naccache, 2001; Sergent et al., 2005).

4.2. Parcellation of the MMN in early and late sub-components

Our findings also led us to distinguish two elementary and distinct neural events within the so-called 'MMN complex', which is usually considered as a homogenous ERP component. We propose to divide the generic 'MMN complex' into an 'early MMN' (~90–160 ms) and a 'late MMN' (~160–220 ms), on the basis of 3 converging results. First, scalp topographies of these two components are markedly different: 'early MMN' corresponds to an anterior negativity surrounded by a posterior and lateral positivity, while 'late MMN' fits with a more central, vertex-centered negativity, preceded by an anterior positivity. Second, their respective cortical sources, estimated through plausible inverse solutions, also differ significantly: 'early MMN' is associated with a focal network centered on auditory regions, while 'late MMN' originates from a more distributed cortical network. Finally, SOA affected the amplitude of 'early MMN', while it only delayed the latency of 'late MMN'. This last difference suggests that 'early MMN' is an echoic auditory memory process with attributes of automaticity, evanescence and modularity, while 'late MMN' would already corresponds to a more central process sensitive to attentional manipulations. This proposal of a parcellation of the MMN may clarify some discrepancies of the literature concerning the relation of MMN to SOA/ISI: indeed, while some studies reported a decrease of MMN amplitude from 2 s to 4 s (Mantysalo & Naatanen, 1987), some others reported a more complex relation with first MMN decreasing from 1.5 s to 2.5 s, then increasing from 2.5 s to 3.5 s (Ermutlu, Demiralp, & Karamursel, 2007).

Note that the late MMN shares many similarities with the N2b component described in the early auditory ERP literature (Snyder & Hillyard, 1976), before the discovery of the MMN (Naatanen, Gaillard, & Mantysalo, 1978) which in turn, progressively led to consider altogether the negativities preceding the P3 complex within a generic "MMN/N2b" component (see for instance: Holeckova, Fischer, Giard, Delpuech, & Morlet, 2006; Neuhaus et al., 2009 for recent illustrations). This trend was also probably reinforced by the description of various subtypes of MMNs with various latencies within a relatively large window between 100 ms and 250 ms after stimulus onset (Naatanen et al., 2001). From this perspective, our rediscovery of the "N2b" component under the name of "late MMN" calls for a more rigorous definition of the negative ERP component of interest in ERP studies, and suggests that this definition has to include a fine functional and/or spatio-temporal description able to distinguish between early and late MMNs.

Indeed, this parcellation of MMN complex may help to resolve current discussions about the automaticity of the MMN. Naatanen et al. initially described the MMN as reflecting an automatic process immune to top-down manipulations, in sharp difference with the P3 complex, and in particular with the P3b component. However a few experimental reports reveal attentional modulation of MMN by spatial attention (Arnott & Alain, 2002) and by the sensory modality used during a dual-task situation (Muller et al., 2002). In close agreement with our proposal (Arnott & Alain, 2002) measured the MMN within a 150–250 ms interval which overlaps mostly with the 'late MMN' window (160–220 ms), as did (Muller et al., 2002) when reporting attentional effects on the MMN in a 100–260 ms interval.

This theoretical proposition calls for additional studies that will test its two principal hypotheses. First, by using more than 3 SOAs, one may better sample the evanescence of early MMN, evaluate whether its decay is exponential (Zylberberg et al., 2009), and test up to which delays the 'late MMN' would still be observed. If 'late MMN' is more related to central processes than to perceptual echoic memory, we predict that it should be elicited under the same conditions as the N2–P3 complex. Mantysalo and Naatanen (1987) reported that MMN was still observed for an ISI of 2 s, and absent at 4 s. However, the use of a better spatial sampling, of a larger range of SOAs and the distinction between early and late components of the MMN may provide new insights on this issue. It is also an open issue to explore if the early and late MMN index strictly serial stages of perception, of if they can overlap in time, as could be expected from serial models implemented with fast feed-forward connections and recurrent processing allowing that onsets of responses at a given stage can occur before the offset of previous stages.

In the same perspective, manipulating subjects attention may help to better distinguish these two ERP components, and to test the hypothesis according to which 'early MMN' should behave as a purely automatic and non conscious process, while 'late MMN' would be more sensitive to executive and attentional control. A first source of evidence supporting our claims comes from a recent study using a different auditory paradigm, based on the detection of auditory regularities both at short (intra-trial, <600 ms) and long (>tens of seconds) time-scales (Bekinschtein et al., 2009). In this study, we could record MMNs from control subjects in various conditions of attention and awareness of auditory stimuli, by means of task and instructions manipulations. We observed an automatic MMN, which was not affected by these manipulations, the topography and cortical sources of which were essentially identical to the 'early MMN' we describe here. This 'early MMN' was even present in patients suffering from comatose of vegetative states, unaware of the surrounding stimuli and unable to perform an active detection task.

Additionally, our finding raises the issue of the generality of this parcellation of the auditory MMN to other sensory modalities: would this proposed distinction between the early activation of an echoic memory network – specific to each sensory modality–, and the late activation of a more central system hold for visual or somatosensory perceptual systems? Or, alternatively would these findings be very specific to the auditory modality? This issue is par-

ticularly difficult because compared to auditory MMN, much less studies are available on other sensory modalities. For instance a few studies explored somatosensory MMN (Kekoni et al., 1997; Shinozaki, Yabe, Sutoh, Hiruma, & Kaneko, 1998) or its magnetic equivalent (Akatsuka, Wasaka, Nakata, Kida, & Kakigi, 2007), and the mere existence of a visual MMN is still a controversial topic (Pazo-Alvarez, Cadaveira, & Amenedo, 2003). In a scalp ERP study, Czigler and Csibra (1992) reported a posterior negative ERP component occurring around 140–180 ms after visual stimulus onset, in a visual oddball paradigm. Importantly, this visual MMN decayed in amplitude when SOA was increased from 340 ms to 1020 ms. However, while the generality of the MMN across sensory modalities is very attractive from a theoretical perspective defining it in terms of Bayesian echoic memory processes (Garrido et al., 2009), several aspects are specific to audition: first, stimulus localization is not coded before informations originating from the two ears converge onto the same neural structure (beginning within the inferior colliculus), while it is coded from the first synaptic relay for vision and somatosensory stimuli. Second, while auditory objects span in time, – typically over several tens of milliseconds–, visual stimuli and to a lesser extent somesthesic stimuli, are usually delivered within a single time frame. Again, these fundamental distinctions may explain very specific properties of the early auditory MMN. In any case, the issue is much clearer concerning the P3 complex and its fMRI equivalent which are engaging a common fronto-parietal network, irrespectively of sensory modality, thus defining it as a common central stage of perception subject to attentional and strategical effects (Ji, Porjesz, Begleiter, & Chorlian, 1999; Linden et al., 1999). Future works will have to test whether the late MMN described in the present study shares these properties with the P3 complex.

4.3. A two-stage serial model of information accumulation for novelty detection

When focusing on the delay effects revealed by our study, we observed a strong relation between 'early MMN' attenuation, and 'late MMN' and P3a and P3b latencies. In particular, P3 onset followed the closure of 'late MMN' component. These two results can be accounted for by an accumulation of evidence model of novelty detection: generic MMN complex could index the progressive accumulation of novelty-related information, followed by a P3 complex when a given threshold of evidence is reached. In this view, the accumulation of evidence could originate from two additional and serial sources respectively indexed by the 'early MMN' and by the 'late MMN'. At short SOAs, the output of the first automatic system would combine with the evidence provided by the second stage, thus increasing the speed and likelihood of attaining a decisional threshold, indexed by the onset of the P3 complex. By contrast, at long SOAs the first stage would not provide any information on novelty detection, due to the fleeting lifetimes of automatic and non-conscious echoic memory representations. In this absence of this initial source of evidence, all successive stages would be delayed. This basic model would provide a new interpretation of MMN, and of its functional significance. The present data is only suggestive of this plausible model, and additional work is needed to test its central hypotheses, and in particular: (1) the proposal of a two-stage versus one stage model; (2) the serial versus parallel nature of information accumulation, and (3) the causal relation between MMN closure and P3 onset. Additionally, we would associate 'early MMN' to a non-conscious stage of processing, while 'late MMN' could already be related to central processes more prone to be consciously accessible. Interestingly, recent works about the timing of conscious access to perceptual representations share the idea of "global workspace theory" by associating this psychological event with the ignition of a largely distributed cortical network, what could suggest that the timing of conscious access might occur even earlier than ~300 ms (P3b temporal window), around ~200 ms and would be indexed by a negativity ERP component (Koivisto, Kainulainen, & Revonsuo, 2009). If 'late MMN' already indexes a consciously accessible (or accessed) representational stage, this could strengthen this line of findings. Future research could address this issue by measuring 'late MMN' responses in relation to subjective reports and other behavioral markers of conscious processing of the auditory stimuli. We could also use a computational approach to test and specify this proposed two-stage model of MMN, inspired by recent neural networks modeling works addressing the distinction between the exponential decay of visual iconic memory representations and their active maintenance within working memory (Zylberberg et al., 2009).

Note also that this parcellation of the MMN complex could also be observed for other dimensions of stimulus deviance than acoustic frequency (e.g.: stimulus duration, stimulus location).

4.4. Clinical perspectives

Finally, we close by a clinically oriented remark. Our work was initially driven by a double motivation: unravelling the distinctions prevailing between auditory novelty detection processes, and use this information to probe these systems in non-communicating humans suffering form disorders of consciousness and related disorders (comatose, VS, MCS, paralyzed patients such as "locked-in patients"). By probing the functionality of novelty detection cognitive processes in these patients and by estimating their resistance to SOA, one may better detect whether the patients are conscious and able to actively keep information in working memory (Bekinschtein et al., 2009). Currently, the presence of an MMN in non-conscious comatose patients has been proven to predict recovery of conscious processing (Fischer et al., 2004; Kane et al., 1993; Naccache et al., 2005). The precise nature of this MMN remains however largely unknown in the light of our findings: does early MMN predict a positive outcome, or is it the later part of it, the presence of which could index a better cognitive status? Could we use the 'late MMN' component as a marker of central cognitive processing? Limited results from Experiment 2 using only two active EEG derivations suggest however that a larger spatial sampling should be used in order to be able to address these issues. Applications of our paradigm to patients may provide new insights in the growing field of clinical neurophysiology of consciousness disorders.

Acknowledgements

This work was supported by the Fondation pour la Recherche Médicale (FRM), the Institut pour le Cerveau et la Moëlle épinière (ICM Institute, Paris, France), INSERM and AP-HP.

The Cartool software (http://brainmapping.unige.ch/Cartool.htm) has been programmed by Denis Brunet, from the Functional Brain Mapping Laboratory, Geneva, Switzerland, and is supported by the Center for Biomedical Imaging (CIBM) of Geneva and Lausanne.

References

Akatsuka, K., Wasaka, T., Nakata, H., Kida, T., & Kakigi, R. (2007). The effect of stimulus probability on the somatosensory mismatch field. *Experimental Brain Research*, *181*(4), 607–614.

Arnott, S. R., & Alain, C. (2002). Stepping out of the spotlight: MMN attenuation as a function of distance from the attended location. *Neuroreport*, *13*(17), 2209–2212.

Atienza, M., Cantero, J. L., & Dominguez-Marin, E. (2002). Mismatch negativity (MMN): An objective measure of sensory memory and long-lasting memories during sleep. *International Journal of Psychophysiology*, *46*(3), 215–225.

Baillet, S., Moscher, J. C., & Leahy, R. M. (2001). Electromgnetic brain mapping. *IEEE Signal Processing. Magazine*, *18*, 14–30.

Bekinschtein, T. A., Dehaene, S., Rohaut, B., Tadel, F., Cohen, L., & Naccache, L. (2009). Neural signature of the conscious processing of auditory regularities. *Proceedings of National Academy of Science USA*, *106*(5), 1672–1677.

Bledowski, C., Prvulovic, D., Hoechstetter, K., Scherg, M., Wibral, M., Goebel, R., et al. (2004). Localizing P300 generators in visual target and distractor processing: A combined event-related potential and functional magnetic resonance imaging study. *Journal of Neuroscience*, *24*(42), 9353–9360.

Clarke, J. M., Halgren, E., & Chauvel, P. (1999). Intracranial ERPs in humans during a lateralized visual oddball task. II. Temporal, parietal, and frontal recordings. *Clinical Neurophysiology*, *110*(7), 1226–1244.

Czigler, I., & Csibra, G. (1992). Event-related potentials and the identification of deviant visual stimuli. *Psychophysiology*, *29*(4), 471–485.

Czigler, I., Csibra, G., & Csontos, A. (1992). Age and inter-stimulus interval effects on event-related potentials to frequent and infrequent auditory stimuli. *Biology and Psychology*, *33*(2–3), 195–206.

Dehaene-Lambertz, G. (2000). Cerebral specialization for speech and non-speech stimuli in infants. *Journal of Cognition Neuroscience*, *12*(3), 449–460.

Dehaene-Lambertz, G., & Dehaene, S. (1994). Speed and cerebral correlates of syllable discrimination in infants. *Nature*, *370*, 292–295.

Dehaene, S., & Naccache, L. (2001). Towards a cognitive neuroscience of consciousness: Basic evidence and a workspace framework. *Cognition*, *79*(1–2), 1–37.

Doeller, C. F., Opitz, B., Mecklinger, A., Krick, C., Reith, W., & Schroger, E. (2003). Prefrontal cortex involvement in preattentive auditory deviance detection: Neuroimaging and electrophysiological evidence. *Neuroimage*, *20*(2), 1270–1282.

Donchin, E., & Coles, M. G. H. (1988). Is the P300 component a manifestation of context updating? *The Behavioral and Brain Sciences*, *11*, 355–372.

Ermutlu, M. N., Demiralp, T., & Karamursel, S. (2007). The effects of interstimulus interval on sensory gating and on preattentive auditory memory in the oddball paradigm. Can magnitude of the sensory gating affect preattentive auditory comparison process? *Neuroscience Letter*, *412*(1), 1–5.

Fischer, C., Luaute, J., Adeleine, P., & Morlet, D. (2004). Predictive value of sensory and cognitive evoked potentials for awakening from coma. *Neurology*, *63*(4), 669–673.

Friston, K. (2005). A theory of cortical responses. *Philosophical Transactions of the Royal Society of London, Series B: Biological Science*, *360*(1456), 815–836.

Garrido, M. I., Kilner, J. M., Stephan, K. E., & Friston, K. J. (2009). The mismatch negativity: A review of underlying mechanisms. *Clinical Neurophysiology*, *120*(3), 453–463.

Giard, M. H., Perrin, F., Pernier, J., & Bouchet, P. (1990). Brain generators implicated in the processing of auditory stimulus deviance: A topographic event-related potential study. *Psychophysiology*, *27*(6), 627–640.

Halgren, E., Marinkovic, K., & Chauvel, P. (1998). Generators of the late cognitive potentials in auditory and visual oddball tasks. *Electroencephalogram Clinical Neurophysiology*, *106*(2), 156–164.

Holeckova, I., Fischer, C., Giard, M. H., Delpuech, C., & Morlet, D. (2006). Brain responses to a subject's own name uttered by a familiar voice. *Brain Research*, *1082*(1), 142–152.

Ji, J., Porjesz, B., Begleiter, H., & Chorlian, D. (1999). P300: The similarities and differences in the scalp distribution of visual and auditory modality. *Brain Topography*, *11*(4), 315–327.

Kane, N. M., Curry, S. H., Butler, S. R., & Cummins, B. H. (1993). Electrophysiological indicator of awakening from coma. *Lancet*, *341*(8846), 688.

Kekoni, J., Hamalainen, H., Saarinen, M., Grohn, J., Reinikainen, K., Lehtokoski, A., et al. (1997). Rate effect and mismatch responses in the somatosensory system: ERP-recordings in humans. *Biology and Psychology*, *46*(2), 125–142.

Koivisto, M., Kainulainen, P., & Revonsuo, A. (2009). The relationship between awareness and attention: Evidence from ERP responses. *Neuropsychologia*, *47*(13), 2891–2899.

Kraus, N., McGee, T. T. L., Nicol, T., & King, C. (1994). Nonprimary auditory thalamic representation of acoustic change. *Journal of Neurophysiology*, *72*(3), 1270–1277.

Laureys, S., Owen, A. M., & Schiff, N. D. (2004). Brain function in coma, vegetative state, and related disorders. *Lancet Neurology*, *3*(9), 537–546.

Levanen, S., Ahonen, A., Hari, R., McEvoy, L., & Sams, M. (1996). Deviant auditory stimuli activate human left and right auditory cortex differently. *Cerebral Cortex*, *6*(2), 288–296.

Levanen, S., Hari, R., McEvoy, L., & Sams, M. (1993). Responses of the human auditory cortex to changes in one versus two stimulus features. *Experimental Brain Research*, *97*(1), 177–183.

Liebenthal, E., Ellingson, M. L., Spanaki, M. V., Prieto, T. E., Ropella, K. M., & Binder, J. R. (2003). Simultaneous ERP and fMRI of the auditory cortex in a passive oddball paradigm. *Neuroimage*, *19*(4), 1395–1404.

Linden, D. E., Prvulovic, D., Formisano, E., Vollinger, M., Zanella, F. E., Goebel, R., et al. (1999). The functional neuroanatomy of target detection: An fMRI study of visual and auditory oddball tasks. *Cerebral Cortex*, *9*(8), 815–823.

Luck, S. J. (2005). *An introduction to the event-related potential technique*. MIT Press.

Mantini, D., Corbetta, M., Perrucci, M. G., Romani, G. L., & Del Gratta, C. (2009). Large-scale brain networks account for sustained and transient activity during target detection. *Neuroimage*, *44*(1), 265–274.

Mantysalo, S., & Naatanen, R. (1987). The duration of a neuronal trace of an auditory stimulus as indicated by event-related potentials. *Biology and Psychology*, *24*(3), 183–195.

Molholm, S., Martinez, A., Ritter, W., Javitt, D. C., & Foxe, J. J. (2005). The neural circuitry of pre-attentive auditory change-detection: An fMRI study of pitch and duration mismatch negativity generators. *Cerebral Cortex*, *15*(5), 545–551.

Muller, B. W., Achenbach, C., Oades, R. D., Bender, S., & Schall, U. (2002). Modulation of mismatch negativity by stimulus deviance and modality of attention. *Neuroreport*, *13*(10), 1317–1320.

Naatanen, R., Tervaniemi, M., Sussman, E., Paavilainen, P., & Winkler, L. (2001). "Primitive intelligence" in the auditory cortex. *Trends in Neuroscience*, *24*(5), 283–288.

Naatanen, R., Gaillard, A. W., & Mantysalo, S. (1978). Early selective-attention effect on evoked potential reinterpreted. *Acta Psychology(Amsterdam)*, *42*(4), 313–329.

Naatanen, R., & Picton, T. (1987). The N1 wave of the human electric and magnetic response to sound: A review and an analysis of the component structure. *Psychophysiology*, *24*(4), 375–425.

Naccache, L., Puybasset, L., Gaillard, R., Serve, E., & Willer, J. C. (2005). Auditory mismatch negativity is a good predictor of awakening in comatose patients: A fast and reliable procedure. *Clinical Neurophysiology*, *116*(4), 988–989.

Neuhaus, A. H., Goldberg, T. E., Hassoun, Y., Bates, J. A., Nassauer, K. W., Sevy, S., et al. (2009). Acute dopamine depletion with branched chain amino acids decreases auditory top-down event-related potentials in healthy subjects. *Schizophrenia Research*, *111*(1–3), 167–173.

Opitz, B., Rinne, T., Mecklinger, A., von Cramon, D. Y., & Schroger, E. (2002). Differential contribution of frontal and temporal cortices to auditory change detection: FMRI and ERP results. *Neuroimage*, *15*(1), 167–174.

Pazo-Alvarez, P., Cadaveira, F., & Amenedo, E. (2003). MMN in the visual modality: A review. *Biology and Psychology*, *63*(3), 199–236.

Perrin, F., Pernier, J., Bertrand, D., & Echallier, J. F. (1989). Spherical splines for scalp potential and current density mapping. *Electroencephalography and Clinical Neurophysiology*, *72*, 184–187.

Polich, J., Eischen, S. E., & Collins, G. E. (1994). P300 from a single auditory stimulus. *Electroencephalography and Clinical Neurophysiology*, *92*(3), 253–261.

Polich, J., & Margala, C. (1997). P300 and probability: Comparison of oddball and single-stimulus paradigms. *International Journal of Psychophysiology*, *25*(2), 169–176.

Restuccia, D., Della Marca, G., Marra, C., Rubino, M., & Valeriani, M. (2005). Attentional load of the primary task influences the frontal but not the temporal generators of mismatch negativity. *Brain Research and Cognitive Brain Research*, *25*(3), 891–899.

Rosburg, T., Trautner, P., Dietl, T., Korzyukov, O. A., Boutros, N. N., Schaller, C., et al. (2005). Subdural recordings of the mismatch negativity (MMN) in patients with focal epilepsy. *Brain*, *128*(Pt 4), 819–828.

Sergent, C., Baillet, S., & Dehaene, S. (2005). Timing of the brain events underlying access to consciousness during the attentional blink. *Nature Neuroscience*, *8*(10), 1391–1400.

Shinozaki, N., Yabe, H., Sutoh, T., Hiruma, T., & Kaneko, S. (1998). Somatosensory automatic responses to deviant stimuli. *Brain Research and Cognitive Brain Research*, *7*(2), 165–171.

Snyder, E., & Hillyard, S. A. (1976). Long-latency evoked potentials to irrelevant, deviant stimuli. *Behavioural Biology*, *16*(3), 319–331.

Squires, N. K., Squires, K. C., & Hillyard, S. A. (1975). Two varieties of long-latency positive waves evoked by unpredictable auditory stimuli in man. *Electroencephalography and Clinical Neurophysiology*, *38*(4), 387–401.

Sutton, S., Braren, M., Zubin, J., & John, E. R. (1965). Evoked-potential correlates of stimulus uncertainty. *Science*, *150*(700), 1187–1188.

Tiitinen, H., May, P., Reinikainen, K., & Naatanen, R. (1994). Attentive novelty detection in humans is governed by pre-attentive sensory memory. *Nature*, *372*(6501), 90–92.

Zylberberg, A., Dehaene, S., Mindlin, G. B., & Sigman, M. (2009). Neurophysiological bases of exponential sensory decay and top-down memory retrieval: A model. *Frontiers in Computational Neuroscience*, *3*, 4.